Cell Reports Medicine, Volume *3*

Supplemental information

A *RET::GRB2* fusion in pheochromocytoma defies the classic paradigm of *RET* oncogenic fusions

Cynthia M. Estrada-Zuniga, Zi-Ming Cheng, Purushoth Ethiraj, Qianjin Guo, Hector Gonzalez-Cantú, Elaina Adderley, Hector Lopez, Bethany N. Landry, Abir Zainal, Neil Aronin, Yanli Ding, Xiaojing Wang, Ricardo C.T. Aguiar, and Patricia L.M. Dahia

Supplementary Information

Table S1- Summary features of the patient cohort, related to STAR Methods.

Table S2- Unique fusion events detected in pheochromocytomas/paragangliomas from RNAseq containing at least three junction reads and one spanning read, related to STAR Methods.

Figure S1- Related to Figure 1

Figure S2- Related to Figure 1

Table S4- Pre-ranked Gene Set Enrichment Analysis of Gene Ontology Pathways (C5 dataset) based on differentially expressed genes (DEGs) between 17 RET mutants and 1 RET::GRB2 fusion tumor and using padjusted <0.05, related to STAR Methods.

Fig S3- Related to Figure 3

Table S5- List of oligonucleotides for PCR and Real Time-PCR, related to STAR Methods

Supplementary Table 1. Summary features of the patient cohort (related to STAR Methods)

Number of patients		52
Median Age (range)		47 (13-78) years
Sex	Female	55%
	Male	45%
Tumor location	Pheochromocytoma	49
	Paraganglioma	3
Hereditary status	Familial	9
	Sporadic	43
Multiplicity	Multiple (including bilateral)	2
	Single	50
Malignancy status	Metastatic	3
	Nonmetastatic	49

Supplementary Table 2. Unique fusion events detected in pheochromocytomas/paragangliomas from RNAseq containing at least three junction reads and one spanning read (related to STAR Methods)

Fusion Name	Junction Read Count	Spanning Fragment Count
RET::GRB2	492	18
CAMK2D::LINC00682	124	15
IL20::TBC1D4	20	1
HDAC5::MFAP5	17	3
TFG::ADGRG7	16	2
TMEM198::SPEG	11	1
ME3::ENTPD3	11	2
FAM162B::GPRC6A	11	1
UBTF::MAML3	10	2
FKBP5::SRPK1	10	1
CD24::RN7SL2	9	4
IGSF21::KCNH1	8	1
CDC5L::TJAP1	8	3
AKAP6::AC097478.1	8	1
LIPA::MARK3	7	3
TIMM10B::RN7SL2	6	1
ITPR2::R3HDM1	6	1
FTO::RN7SL2	5	1
FRY::PDLIM5	5	1
FAM135B::AL137230.1	5	2
APOPT1::REXO1	5	1

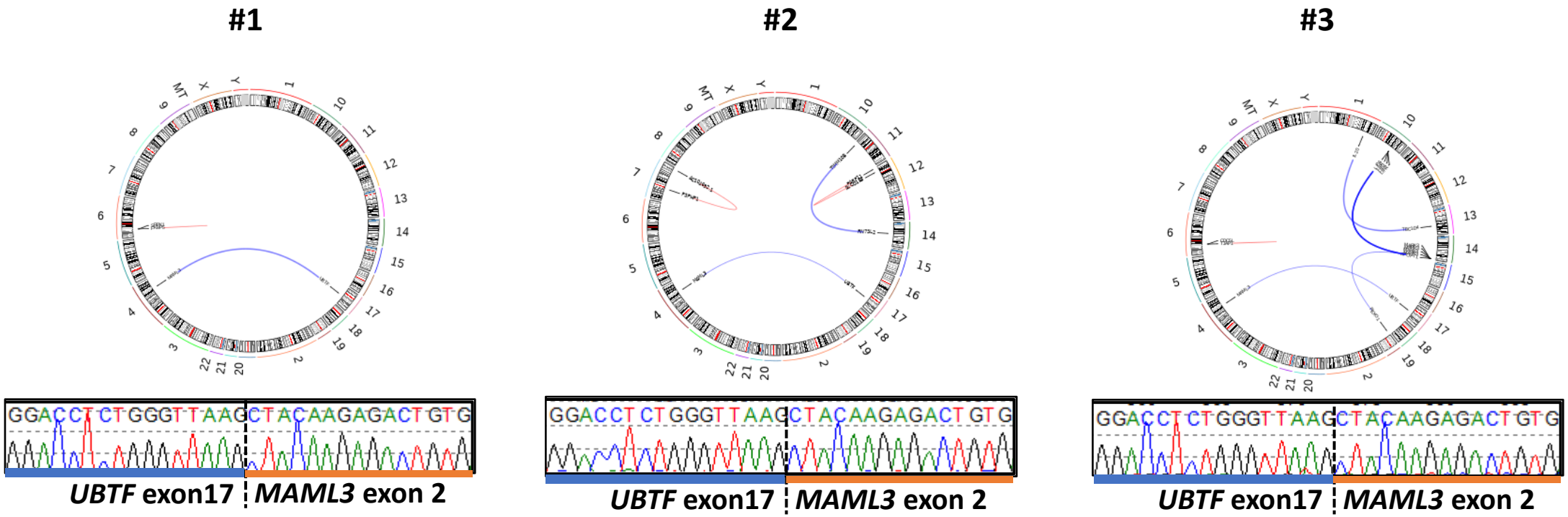

Figure S1. Known gene fusions in pheochromocytomas and paragangliomas. Chromosomes plotted as ideograms around the outside of the circle (CIRCOS) plot of three independent pheochromocytomas without a known driver event depicting predicted *UBTF-MAML3* fusions, which were confirmed by independent RT-PCR and Sanger sequencing of tumor cDNA (bottom) and shown to carry an identical hybrid transcript. Related to Figure 1.

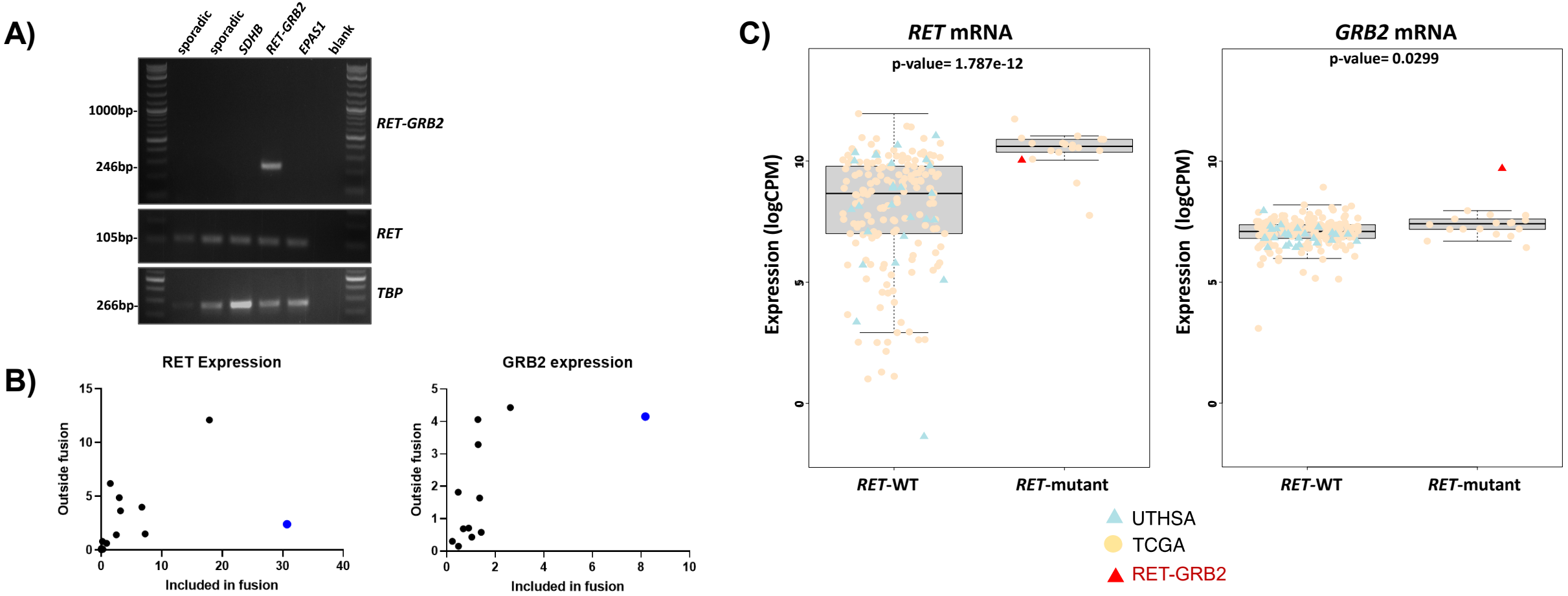

Fig S2. Validation of RET-GRB2 fusion in a pheochromocytoma A) Agarose gel electrophoresis of products of three PCRs of *RET-GRB2*, *RET* wild-type and *TBP* (housekeeping control) transcripts. Templates were cDNAs from four composite tumors (lanes 1-4): three ganglioneuroma/pheochromocytoma (lanes 1, 2 and 4) and one paraganglioma/ganglioneuroma (lane 3), and an additional pheochromocytoma used as control (lane 5) and a no cDNA control for the PCR ('blank). The tumor genotypes are indicated (lanes 1-5): two tumors have no identified driver mutation ('sporadic', lanes 1 and 2), one has a germline *SDHB* mutation (lane 3), the *RET-GRB2*-fusion positive tumor was a positive control (lane 4), and a pheochromocytoma with *EPAS1* mutation was a negative control (lane 5). **B**) Quantitative real time PCR of cDNA of RET (left) and GRB2 (right) of pheochromocytomas/paragangliomas of known genotypes, including RET mutants and the tumor carrying the RET-GRB2 fusion (blue dot) depicting an exon within the fusion (x axis) plotted against an exon not involved in the fusion (y axis). The tumor with RET-GRB2 fusion shows disproportionally higher expression of the exons spanned by the fusion, replicating the findings of the RNAseq cohort (related to Fig.1F). **C)** *RET* and *GRB2* mRNA from combined datasets of our RNAseq cohort (UTHSA, n=30) and the TCGA pheochromocytoma-paraganglioma cohort (TCGA, n=178) displayed based on *RET* genotype (wild-type= *RET*-WT or mutant= *RET* mutant). The *RET-GRB2* fusion-positive tumor displayed *RET* transcription levels within the range of *RET* mutant PPGLs, and higher than those of *RET* wild-type tumors. The *RET-GRB2* fusion-expressing tumor was the top expressor of *GRB2* mRNA. Related to Figure 1.

Supplementary Table 4. Pre-ranked Gene Set Enrichment Analysis of Gene Ontology Pathways (C5 dataset) based on differentially expressed genes (DEGs) between 17 RET mutants and 1 RET::GRB2 fusion tumor and using padjusted <0.05 (related to STAR Methods)

GS DETAILS	ES	NES	NOM p-val	FDR q-val	FWER p-val	RANK AT MAX	LEADING EDGE
GOBP_POSITIVE_REGULATION_OF_TRANSCRIPTION_BY_RNA_POLYMERASE_II	18	-0.48	-1.4	0.092	0.902	0.351	10
GOMF_IDENTICAL_PROTEIN_BINDING	20	-0.46	-1.38	0.11	0.502	0.379	39
GOBP_POSITIVE_REGULATION_OF_BIOSYNTHETIC_PROCESS	21	-0.44	-1.36	0.112	0.373	0.415	10
GOBP_POSITIVE_REGULATION_OF_NUCLEOBASE_CONTAINING_COMPOUND_METABOLIC_PROCESS	23	-0.42	-1.36	0.105	0.281	0.415	10
GOMF_CIS_REGULATORY_REGION_SEQUENCE_SPECIFIC_DNA_BINDING	45	-0.26	-0.92	0.603	1	0.965	4
GOMF_DNA_BINDING_TRANSCRIPTION_FACTOR_ACTIVITY	52	-0.21	-0.8	0.813	1	0.992	4
GOBP_NEGATIVE_REGULATION_OF_BIOSYNTHETIC_PROCESS	15	-0.28	-0.8	0.729	1	0.992	4
GOMF_SEQUENCE_SPECIFIC_DNA_BINDING	52	-0.21	-0.79	0.845	1	0.992	4
GOMF_TRANSCRIPTION_REGULATOR_ACTIVITY	55	-0.21	-0.77	0.864	0.983	0.995	4
GOBP_NEGATIVE_REGULATION_OF_NUCLEOBASE_CONTAINING_COMPOUND_METABOLIC_PROCESS	18	-0.25	-0.75	0.8	0.905	0.996	4
GOCC_CHROMOSOME	20	-0.22	-0.68	0.884	0.896	0.999	4

GOBP=gene ontology, biological process; GOMF=gene ontology molecular function; GOCC=gene ontology cell compartment; ES= enrichment score; NES=normalized enrichment score; NOM=nominal pvalue; FDR=false discovery rate; Familywise-error rate; Rank at Max=the position in the ranked list at which the maximum enrichment score occurred; leading edge- percentage of genes in the pathway contributing to the enrichment score.

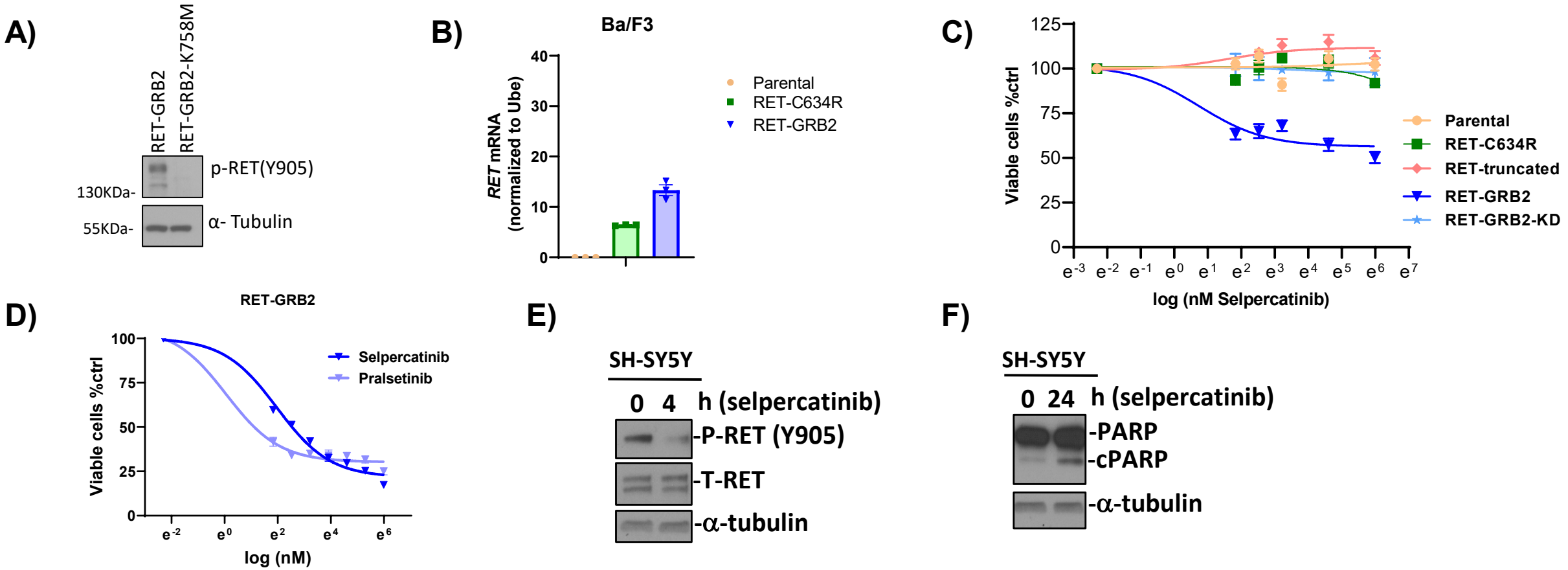

Fig S3. RET-GRB2 fusion sensitivity to RET inhibitors. **A)** Western blot of lysates from Ba/F3 cells expressing RET-GRB2 or RET-GRB2 kinase dead (KD, carrying a K758M mutation) probed with phosphorylated RET (Y905), tubulin is a loading control; three biological replicates were performed; **B)** Quantitative real time PCR of human RET in cDNA from Ba/F3 cell lines stably expressing the designated constructs. Primers were designed to span a region of the *RET* transcript included in all constructs (exons 4 and 5). Mouse *Ube* was used as a housekeeping control. Samples were run in triplicates and two biological repeats were performed; **C)** Growth rate of Ba/F3 cells stably expressing the indicated constructs or parental cells seeded at 2.5 x 10^5 cells per well in triplicate and cultured in the presence of interleukin 3 (IL3). Cells were counted daily for four days. Three biological replicates were performed. Under these conditions, selpercatinib did not inhibit the growth of parental cells or cells expressing truncated RET or kinase dead RET-GRB2 fusion and was also significantly less effective towards RET-GRB2 expressing cells IC50=114nM (95% CI=37-361nM); three biological replicates were performed; **D)** IC50 concentration–response curves to selpercatinib (18.3nM, 95%CI=13-25nM) or pralsetinib (10.1nM, 95%CI=5-19nM) at doses of 0, 6.25, 12.5, 25, 50, 100 and 200nM for 72h measuring inhibition of growth of Ba/F3 cells expressing the *RET-GRB2* fusion seeded in triplicate per each dose and drug, repeated in three biological replicates; **E)** Western blots of lysates from SH-SY5Y cells expressing RET-GRB2 and treated with 50nM selpercatinib were probed with phosphorylated RET (Y905) and total RET, tubulin is the loading control, two technical replicates were performed; **F)** Western blots of lysates from SH-SY5Y cells RET-GRB2 and treated with 50nM selpercatinib were probed with PARP and cleaved PARP(c-PARP), α-tubulin is a loading control, two technical replicates were performed. Related to Figure 3.

Supplementary Table 5. List of oligonucleotides for PCR and Real Time-PCR (related to STAR Methods)

Oligonucleotide name and sequence	**Source**	**Identifier**
Primer: GRB2_e1_cDNA_F Forward: F GGCCACTGCTCTTAATCGTC	This paper	N/A
Primer: GRB2_e1_cDNA_R Reverse: GTCTTCCCTGCTGAAGCAAC	This paper	N/A
Primer: GRB2_e5_cDNA_F Forward: TCCTCTGGGTGGTGAAGTTC	This paper	N/A
Primer: GRB2_e6_cDNA_R Reverse: AAGCTCCTTTCCACCAGTTG	This paper	N/A
Primer: RET_e11_genDNA_F Forward: GTGCCAAGCCTCACACCAC	This paper	N/A
Primer: RET_e11_genDNA_R Reverse: CCTCCGGAAGGTCATCTCAG	This paper	N/A
Primer: RET_e19_genDNA_F Forward: TAGTTGTGGCACATGGCTTG R	This paper	N/A
Primer: RET_e19_genDNA_R Reverse: AGGCCGTCGTCATAAATCAG	This paper	N/A
Primer: GRB2_e1_genDNA_F Forward: GGCCACTGCTCTTAATCGTC	This paper	N/A
Primer: GRB2_e1_genDNA_R Reverse: GTCTTCCCTGCTGAAGCAAC	This paper	N/A
Primer: GRB2_e5_genDNA_F Forward: TTAGAGCCTTTAGCCGGTCA	This paper	N/A
Primer: GRB2_e5_genDNA_R Reverse: GAACTTCACCACCCAGAGG A	This paper	N/A
Primer (mouse sequence): Ube2d1_F CCCGTGGGAGATGACTTGTTC	This paper	N/A
Primer (mouse sequence) Ube2d1_R GGATAGTCTGTCGGAAAGTGGA	This paper	N/A